Uncertainties in Reactor Neutrino Fluxes and in the Anomaly

A.C. Hayes
[1] *Theoretical Division, Los Alamos National Laboratory, Los Alamos, New Mexico, 87545, USA*

We examine the uncertainties in reactor neutrino fluxes within a nuclear physics framework. These uncertainties enter any analysis of the reactor neutrino anomaly, wherein it is suggested that only about 94% of the emitted antineutrino flux was detected in short baseline experiments. We find that the form of the corrections that lead to the anomaly are very uncertain for the 30% of the flux that arises from forbidden beta decays. Given the present lack of detailed knowledge of the structure of the forbidden transitions, it is difficult to convert the measured aggregate fission beta spectra to antineutrino spectra to the accuracy needed to infer an anomaly. In addition, we analyze the shoulder in the antineutrino spectra observed in current reactor experiments within a nuclear database framework. We find that the ENDF/B-VII.1 database predicts that the antineutrino shoulder arises from an analogous shoulder in the aggregate fission beta spectra. In contrast, the JEFF-3.1.1 database does not predict a shoulder. We consider several possible origins of the shoulder, and find possible explanations. For example, there could be a problem with the measured aggregate beta spectra, or the harder neutron spectrum at a light-water power reactor could affect the distribution of beta-decaying isotopes. In addition to the fissile actinides, we find that ^{238}U could also play a significant role in distorting the total antineutrino spectrum. Distinguishing these and quantifying whether there is an anomaly associated with measured reactor neutrino signals will require new short-baseline experiments, both at thermal reactors and at reactors with a sizable epithermal neutron component.

1 Introduction

There are currently two puzzles associated with measured reactor antineutrino spectra: (1) the magnitude of the spectra measured in all short-baseline experiments is lower than current models, and (2) the shape of the measured spectra deviate from these model predictions. The first of these puzzles is normally termed [1] the "reactor neutrino anomaly", and it generally refers to a 3σ deficit in the number of antineutrinos detected in short-baseline reactor neutrino experiments relative to the number predicted. The second puzzle is that the shape of the antineutrino spectra measured in the near detectors of both Daya Bay [2] and RENO [3] are not consistent with the antineutrino spectrum predictions [4,5] that we refer to as the Huber-Mueller model. Most notably, the measured antineutrino spectra exhibit a significant shoulder relative to the model predictions at antineutrino energies $E_\nu \approx 5-7$ MeV. The spectra measured at Daya Bay [2], RENO [3], and Double Chooz [6] all exhibit this shoulder. We note that the two antineutrino flux puzzles are not necessarily related.

The antineutrino spectrum emitted from a reactor is determined by [7] the reactor thermal power (W_{th}), the energy released in fission by each actinide (e_i), the fractional contribution (f_i/F, $F = \Sigma_i f_i$) of each actinide to the fissions taking place, and the antineutrino spectrum

for each actinide $S_i(E_i)$.

$$S(E_\nu) = \frac{W_{th}}{\Sigma_i (f_i/F) e_i} \Sigma_i (f_i/F) S_i(E_\nu). \quad (1)$$

The thermal power and the fission fractions are both functions of time and are supplied by the reactor operator, while the energy contributing to the thermal power per fission of each actinide (e_i) is normally taken from refs.[8,9]. The Daya Bay near-detector has provided an absolute determination of the reactor antineutrino flux, and this is consistent in magnitude with the previous world average short-baseline reactor neutrino experiments. As such, the measured magnitude is consistent with an anomalous deficit with respect to the most recent estimates [4,5] of the expected reactor antineutrino flux. The spectral distortions and the shape of the shoulder seen in current experiments cannot be produced by any standard L/E dependence required of neutrino oscillations, sterile or otherwise. Thus, there is a need to investigate uncertainties in the antineutrino spectra within a detailed nuclear physics framework.

2 The Corrections to beta-decay that led to the anomaly

There is extensive literature dealing with the reactor anomaly, starting with a seminal paper by Mueller *et al.* [5] that reexamined the reactor antineutrino flux. The latter publication sought to improve the earlier flux estimates based on the ILL on-line measurements [10,11] of the integral beta spectrum of the fission products. The improvements [1,5] on the earlier analyses of ILL integral measurements led to an increased energy of the antineutrino flux, which was subsequently verified in an independent analysis [4].

The beta-decay spectrum S for a single transition in nucleus (Z, A) with end-point energy $E_0 = E_e + E_\nu$ is

$$S(E_e, Z, A) = S_0(E_e) F(E_e, Z, A) C(E_e) (1 + \delta(E_e, Z, A)) \,, \quad (2)$$

where $S_0 = G_F^2\, p_e E_e (E_0 - E_e)^2 / 2\pi^3$, $E_e(p_e)$ is the electron total energy (momentum), $F(E_e, Z, A)$ is the Fermi function needed to account for the Coulomb interaction of the outgoing electron with the charge of the daughter nucleus, and $C(E_e)$ is a shape factor [12] for forbidden transitions due to additional lepton momentum terms. For allowed transitions $C(E) = 1$. The term $\delta(E_e, Z, A)$ represents fractional corrections to the spectrum that were the central focus of the original anomaly studies. The primary corrections to beta decay are radiative, finite size, and weak magnetism, or $\delta(E_e, Z, A) = \delta_{\rm rad} + \delta_{\rm FS} + \delta_{\rm WM}$.

Before discussing the details of the corrections $C(E_e)$ and $\delta(E_e)$, we briefly summarize the treatments used in earlier work. The radiative corrections as derived by Sirlin [13] were included in the description of the beta spectra (though not in the antineutrino spectra) in the original analyses of Schreckenbach *et al.* [10,11]. In the later ILL work [11] an approximation for the FS and WM corrections was included by first deducing the antineutrino spectrum from the measured beta spectra without these corrections, and then applying a linear correction to the deduced antineutrino spectrum of the form, $\delta_{\rm FS} + \delta_{\rm WM} = 0.0065(E_\nu - 4\ {\rm MeV})$. In that work no corrections were made for the shape factors $C(E_e)$. In other analyses [5,4,14] an approximation (derived by Vogel [15]) for the FS and WM corrections was applied on a transition-by-transition basis and the shape factor appropriate for unique forbidden transitions was used for all forbidden transitions. In the present work, we derived *ab initio* analytic expressions for the FS and WM corrections for allowed GT transitions, as well as WM and shape factors for first-forbidden GT operators. We used the radiative corrections derived by Sirlin [13].

We now turn to the form of the corrections. The attractive Coulomb interaction *increases* the electron density near the nuclear surface and increases the beta-decay rate, while the finite nuclear size *decreases* the electron density and decreases the rate (relative to the point-nucleus Fermi function). Using first-order perturbation theory in $Z\alpha$, the finite-size correction to the

Table 1: The shape factors and leading-order weak magnetism corrections to allowed and first-forbidden Gamow-Teller beta decays are shown in the top panel. The shape factors for allowed and first-forbidden Fermi beta decays are shown in the bottom panel. All agree with Ref. [20] for $Z = 0$. The weak magnetism correction for $\vec{J}_V$ involves the unknown overlap of very different 1^- matrix elements and is therefore not listed. The nucleon isovector magnetic moment is $\mu_v = 4.7$, M_N is the nucleon mass, g_A is the axial vector coupling constant, and $\beta = p_e/E_e$. No meson currents were used in the magnetic moment operator, and a truncated orbital current led to the factor of "1/2" in $\delta_{\rm WM}$.

Classification	Operator	Shape Factor $C(E_e)$	$\delta_{\rm WM}(E_e)$
Allowed GT	$\Sigma \equiv \sigma\tau$	1	$\frac{2}{3}\left[\frac{\mu_v - 1/2}{M_N g_A}\right](E_e\beta^2 - E_\nu)$
1^{st} For. GT	$[\Sigma, r]^{0-}$	$p_e^2 + E_\nu^2 + 2\beta^2 E_\nu E_e$	0
1^{st} For. ρ_A	$[\Sigma, r]^{0-}$	$\lambda\, E_0^2$	0
1^{st} For. GT	$[\Sigma, r]^{1-}$	$p_e^2 + E_\nu^2 - \frac{4}{3}\beta^2 E_\nu E_e$	$\left[\frac{\mu_v - 1/2}{M_N g_A}\right]\left[\frac{(p_e^2+E_\nu^2)(\beta^2 E_e - E\nu) + 2\beta^2 E_e E_\nu (E_\nu - E_e)/3}{(p_e^2 + E_\nu^2 - 4\beta^2 E_\nu E_e/3)}\right]$
1^{st} For. GT	$[\Sigma, r]^{2-}$	$p_e^2 + E_\nu^2$	$\frac{3}{5}\left[\frac{\mu_v - 1/2}{M_N g_A}\right]\left[\frac{(p_e^2+E_\nu^2)(\beta^2 E_e - E\nu) + 2\beta^2 E_e E_\nu (E_\nu - E_e)/3}{(p_e^2 + E_\nu^2)}\right]$
Allowed F	τ	1	0
1^{st} For. F	$r\tau$	$p_e^2 + E_\nu^2 + \frac{2}{3}\beta^2 E_\nu E_e$	0
1^{st} For. $\vec{J}_V$	$r\tau$	E_0^2	-

Fermi function, $\delta_{\rm FS}$, for allowed GT transitions is [16]

$$\delta_{\rm FS} = -\frac{3}{2}\frac{Z\alpha}{\hbar c}\langle r\rangle_{(2)}\left(E_e - \frac{E_\nu}{27} + \frac{m_e^2 c^4}{3E_e}\right) \quad . \tag{3}$$

The quantity $\langle r\rangle_{(2)} = \int d^3r\, \rho_W(r) \int d^3s\, \rho_{\rm ch}(s) \mid \vec{r} - \vec{s} \mid$ is the first moment of the convoluted nuclear weak and charge densities (called a Zemach moment [17]). We assume uniform distributions of radius R for the weak and charge densities, for which [18] $\langle r\rangle_{(2)} = \frac{36}{35}R$.

The WM correction arises from the interference of the magnetic moment distribution of the vector current, $\vec{J}_V = \vec{\nabla} \times \vec{\mu}$, with the spin distribution $\vec{\Sigma}$ of the axial current. We previously derived [16] the WM corrections for allowed and first-forbidden operators. There are four possible operators in the case of first-forbidden GT transitions, and all have well-defined WM corrections, as listed in Table 1. Our [16] FS and WM corrections for allowed GT transitions are identical to those derived by Holstein [19], but differ from the forms used in other work [5,4,14,15]. The first-forbidden shape factors, $C(E_e)$, n Table 1 agree with the forms derived by Millener[20] in the $Z = 0$ limit.

3 The antineutrino spectrum dependence on forbidden transitions

To examine the effect of the forbidden beta-decay transitions on the expected antineutrino spectrum we fitted the Schreckenbach [11] electron spectrum, with and without a treatment for forbidden decays. There is no unique physical prescription for beta-decay operator assignments to the transitions included in the fit. For this reason we examined four prescriptions: (1) all transitions are assumed to be allowed; (2) all end-point energies can be associated with either an allowed or forbidden transition; (3) 30% of the branches are selected to be forbidden at equal energy intervals; (4) 30% of the branches are selected to be forbidden with a bias towards higher energies. In addition, we examine fits in which the operator determining the forbidden decays was taken to be $[\Sigma, r]^{0-}$, $[\Sigma, r]^{1-}$, $[\Sigma, r]^{2-}$ or a combination of these. We found excellent fits to the electron spectrum in all cases. However, different treatments of the forbidden transitions

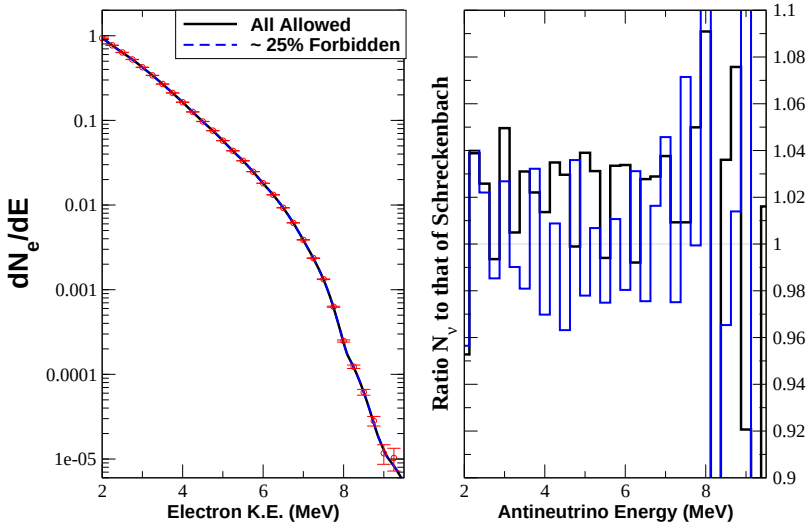

Figure 1 – The fit to the electron spectrum for ^{235}U (left) for two different assumptions on how to treat forbidden transitions, and the ratio of the corresponding antineutrino spectra to that of Schreckenbach (right). The electron spectra are fit assuming (a) all allowed GT branches, or (b) up to 30% forbidden GT transitions. In both cases the WM and FS corrections are included. When folded over the neutrino detection cross section, the case for all allowed (25% forbidden) transitions results in a 2.2% (0.06%) increase in the number of detectable antineutrinos.

can lead to antineutrino spectra that differ both in shape and magnitude at about the 4% level. Two examples are shown in Fig.1, where we present the fits obtained when the WM and FS corrections are included. In one case all transitions are assumed to be allowed, while in the second case the best fit results from about 25% forbidden decays. For the assumption of all allowed transitions, we see a systematic increase of about 2.2% in the number of antineutrinos relative to Schreckenbach, while including forbidden transitions leads to no increase relative to Schreckenbach.

4 The Shoulder

We calculated the aggregate beta and antineutrino spectra using both the ENDFB/V-II.1 [21] and JEFF-3.1.1 [22] nuclear data libraries that provide cumulative yields Y_{F_i} for all fission fragments of interest. The updated ENDF/B-VII.1 beta-decay library [23,24] provides spectra for approximately 95% of the nuclei appearing in eq.(2). The remaining 5% of the fission fragments are modeled [25,26] by extension of the Finite-Range Droplet Model plus Quasi-particle Random Phase Approximation (QRPA). Figure (2) shows the database predictions for the shape of the antineutrino spectra for Daya Bay [27] and RENO [28] relative to the Huber-Mueller model [4,5]. The Daya Bay and RENO experiments differ in the linear combination of actinides determining the total fissions. For Daya Bay the ^{235}U: ^{238}U: ^{239}Pu: ^{241}Pu fission split is 0.586: 0.076: 0.288: 0.05. RENO has not published their fission split, but we took 0.62: 0.12: 0.21: 0.05 from Kim [28]. As can be seen in Fig. (2), the ENDF/B-VII.1 fission fragment yields lead to the prediction of a shoulder relative to the Huber-Mueller model, but the JEFF-3.1.1 yields do not. This striking difference arises because the cumulative fission yields for some nuclei that dominate in the shoulder region are different in the two evaluations. Within the ENDF/B-VII.1 analysis, the shoulder in the antineutrino spectrum results from a corresponding shoulder in the aggregate beta spectrum, and involves the decay of several nuclei, as listed in Dwyer and Langford [29]. We next discuss in detail possible origins of the shoulder.

1. Non-fission sources of antineutrinos: We examined the contribution to the antineutrino spec-

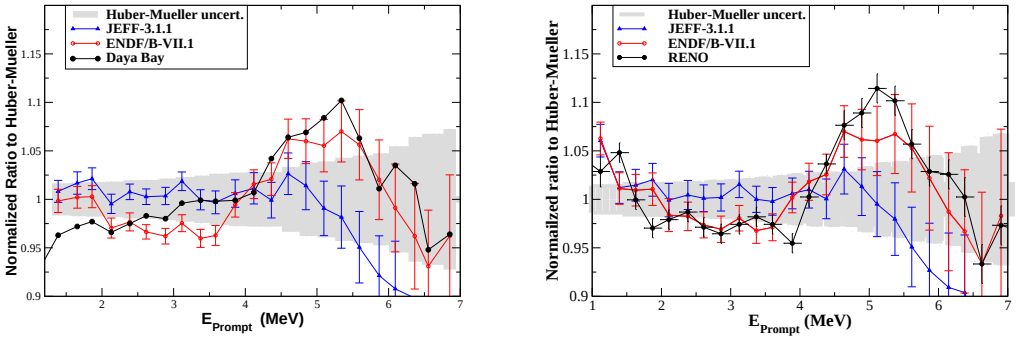

Figure 2 – The ENDF/B-VII.1 and JEFF-3.1.1 predictions for the ratio of the Daya Bay and RENO antineutrino spectra to the Huber-Mueller model. In all cases, the spectra are normalized to the same number of detectable antineutrinos in the energy window $E_\nu = 2-8$ MeV as the Huber-Mueller spectra when folded over the antineutrino detection cross section. The database uncertainties shown are only for the beta-decay branches. The uncertainties arising from the fission-fragment yields are large, as is evident from the difference between the ENDF/B-VII.1 and JEFF-3.1.1 predictions. The large difference between the two database predictions for the shoulder arises entirely from a difference in the evaluated fission fragment yields.

trum from neutron-induced reactions in reactor materials other than the fuel. We used MCNP simulations that are available for all neutron-induced reactions on the coolant, cladding, and structural materials in the NRU CANDU reactor at Chalk River. We then calculated the expected beta-decay spectrum from the unstable nuclei produced by these reactions. We found that all of the antineutrinos from this source are well below the energy of the shoulder. While materials in other reactors may differ in detail from those at the NRU reactor, none is known to produce a significant number of antineutrinos above 2 MeV, and we conclude that non-actinide sources of antineutrinos cannot explain the shoulder.

2. The forbidden nature of transitions: Several of the beta-decay transitions involving ^{96,98}Y, ^{90,92}Rb, and ^{142}Cs that dominate in the shoulder region have a total angular momentum and parity change that generates no weak-magnetism correction [16]. This fact was not taken into account in the analyses of Huber [4], Mueller [5], or Fallot [14]. Above half of the end-point energy in an allowed decay, the weak-magnetism contribution reduces the antineutrino component. This is opposite in sign to the other leading corrections [4,5,16] that suggested the existence of the reactor anomaly [1]. Thus, the lack of a weak-magnetism correction for $0^+ \rightarrow 0^-$ transitions increases the magnitude of the antineutrino flux relative to the Huber-Mueller model. A second issue is that the shape factor, $C(E)$, associated with $0^+ \rightarrow 0^-$ forbidden transitions [16] is quite different from the approximation used by Mueller *et al.* [5], who took the shape factor for all forbidden transitions to be that for a unique forbidden transition. A third issue is the lack of a proper finite-size Coulomb correction to the Fermi function for these transitions [16], where all analyses to-date (including the present one) were forced to use an approximation.

We calculated the antineutrino spectra with and without taking the $\Delta J^{\Delta\pi} = 0^-$ nature of transitions into account. There are two possible shape factors for such transitions [16] that affect the spectrum differently, which introduces an uncertainty in the shape of the aggregate antineutrino spectrum. Using the shape factor that gives the bigger increase in the antineutrino spectrum and setting the weak-magnetism term to zero, we found an increase in the shoulder region of less than 1%. We conclude that a proper treatment of forbidden transitions cannot account for a significant fraction of the shoulder.

3. ^{238}U as a source of the shoulder: RENO reports that ^{238}U is responsible for about 12% of its fissions, while Daya Bay reports only 7.6%. Referring to Fig. (2), relative to their respective experimentally established base lines (rather than with respect to Huber-Muller), the RENO shoulder is more than 50% larger than that observed at Daya Bay. This raises the question

whether ^{238}U, which was not measured in the original ILL experiments [10,11], could be causing the shoulder. Because ^{238}U fissions into isotopes further off the line of stability than ^{235}U, its antineutrino spectrum is both larger and harder in energy, and in the region $E_{\rm prompt} = 4 - 6$ MeV the ^{238}U spectrum is almost twice as large as that of ^{235}U. Thus, ^{238}U contributes about 24% (15%) to the total spectrum in the shoulder region for RENO (Daya Bay). We compared the ENDF/B-VII-1 and JEFF-3.1.1 predictions for ^{238}U to Mueller's prediction [5], and found that both databases predict a significant shoulder for ^{238}U. The magnitude of the JEFF-3.1.1 (ENDF/B-VII.1) shoulder and the percentage contribution to the total antineutrino spectrum suggests that ^{238}U could account for 25% (50%) of the observed shoulder in RENO and Daya Bay. To account for the entire shoulder the ^{238}U yields of the fission products dominating the shoulder region would have to be on average about a factor of four (two) larger than the JEFF-3.1.1 (ENDF/B-VII.1) evaluations. While not ruled out, this is unlikely. Thus, we conclude that ^{238}U could be responsible for a significant fraction of the observed shoulder, but probably not the entire shoulder.

4. The relatively harder PWR Neutron Spectrum: The neutron flux spectra at the PWR reactors used by Daya Bay, RENO and Double Chooz are harder in energy than the thermal spectrum of the ILL reactor, and involve considerably larger epithermal components. This raises the question whether epithermal neutron contributions to the fission of ^{235}U, ^{239}Pu and ^{241}Pu could result in a shoulder in the antineutrino spectrum. Studies [30] of energy-dependent variations in the fission product yields found clear evidence for significant yield changes for nuclei in the valley of the double-humped mass-yield curve. For example, the epithermal yield (relative to thermal) for the relatively unimportant isotope ^{115}Cd varies by a factor of 0.5-3.0, depending on the location of epithermal fission resonances. The effects are much more pronounced in ^{239}Pu than in ^{235}U. Resonance-to-resonance fluctuations cause the *average* effect to be small ($\sim 4\%$) in the energy range $19 < E_n < 61$ eV for ^{235}U, while in ^{239}Pu the prominent and isolated resonance at 0.3 eV produces a change in the ^{115}Cd yield of more than a factor of two. For high-yield fission products, such as ^{96}Y and ^{92}Rb, yield changes are not expected to be as large as for nuclei like ^{115}Cd, both because of theoretical arguments [31] and because the sum of the independent yields is fixed. But changes of the order of 20% are not ruled out. A comparison of the antineutrino spectrum measured at a very thermal reactor with that at a reactor with a sizable epithermal neutron component would be valuable in addressing this issue.

5. A possible error in the ILL beta-decay measurements: As pointed out by Dwyer and Langford [29] the ENDF/B-VII.1 prediction of a shoulder in the antineutrino spectrum in Fig. (2) corresponds to an analogous shoulder in the aggregate beta spectrum. In Fig. (3) we show the absolute ratio of the ENDF/B-VII.1 prediction for the aggregate beta spectrum for ^{235}U to that of Schreckenbach [10,11]. We conclude that the shoulder could be the result of a problem in the measurement or analysis of the beta-spectrum measurements at ILL.

Finally, we comment on whether database analyses of the antineutrino spectra provide any insight on the reactor neutrino anomaly [1]. The most important comment is that the database uncertainties are too large to draw any conclusions. Nonetheless, it is noteworthy that in comparing the two fission-yield evaluations, the prediction of a shoulder (no shoulder) appears to be correlated with the predictions of no anomaly (an anomaly). Daya Bay observes a shoulder and its measured absolute rate is in excellent agreement [27] with the previous world average. The ENDF/B-VII.1 prediction for both the shoulder and the absolute magnitude of the antineutrino spectrum are close to Daya Bay; that is, relative to ENDF/B-VII.1, Daya Bay sees no anomaly. In contrast, the JEFF-3.1.1 predictions are closer to the Huber-Mueller model, which would suggest an anomaly.

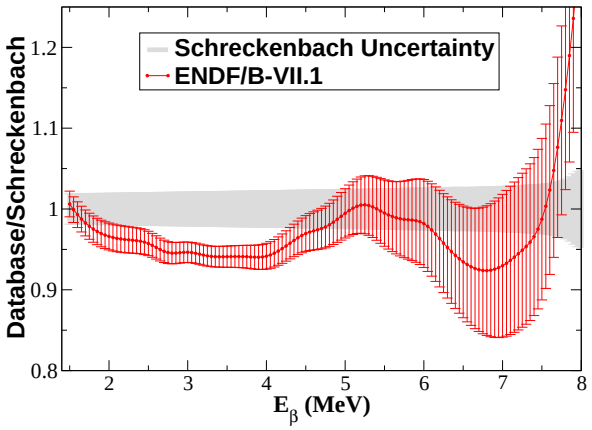

Figure 3 – . The absolute ratio of the ENDF/B-VII.1 aggregate beta spectrum for ^{235}U to that of Schreckenbach. The shoulder in the energy window $E_\beta \approx 4-6$ MeV corresponds to the same shoulder in the ENDF/B-VII.1 antineutrino spectrum shown in Fig. (2).

5 The Need for New Experiments

Both the anomaly and the shoulder could be due to (a) a difference in the hardness of the reactor neutron spectrum, or (b) a problem with the original aggregate beta-spectra measurement [10,11] at the ILL. It is also possible that the shoulder and the anomaly are not correlated. Answering these questions is not possible within current theoretical frameworks or from existing data. Consequently a new set of reactor experiments is needed at short baselines. To address the important issue of the anomaly and the possible existence of a 1 eV sterile neutrino, two detectors at different distances viewing the same reactor are needed. To quantify the role of the neutron spectrum on the shape and magnitude of the antineutrino spectrum, one measurement should be carried out at a very thermal reactor and the other at a reactor with a considerably harder neutron spectrum. The use of highly enriched ^{235}U fuel has the advantage of restricting the resulting antineutrino flux to fragments produced by a single actinide. On the other hand, if ^{238}U and/or ^{239}Pu play a significant role in the anomaly or the shoulder, measurements from fuel that is of low enrichment will be needed to reduce these sources of uncertainty.

References

1. G. Mention *et al.*, *Phys. Rev. D* **83** 073006 (2011).
2. F. P. An *et al.*, *Phys. Rev. Lett.* **108**, 171803 (2012).
3. J. K. Ahn *et al.*, *Phys. Rev. Lett.* **108**, 191802 (2012).
4. P. Huber, *Phys. Rev. C* **84**, 024617 (2011).
5. Th. A. Mueller *et al.*, *Phys. Rev. C* **83**, 054615 (2011).
6. Y. Abe *et al.*, *Phys. Rev. Lett.* **108**, 131801 (2012).
7. Jun Cao, *Nucl. Phys. B Proc. Supp.* **229-232**, 205 (2012).
8. M. F. James, *J. Nucl. Energy* **23**, 517 (1969).
9. V. Kopeikin, L. Mikaelyan, and V. Sinev, *Phys. Atom. Nucl.* **67**, 1892 (2004); *Yad. Fiz.* **67** 1916 (2004).
10. K. Schreckenbach, H. R. Faust, F. von Feilitzsch, A. A. Hahn, K. Hawerkamp, and J. L. Vuilleumier, *Phys. Lett.* **99B**, 251 (1981); F. von Feilitzsch, A. A. Hahn, and K. Schreckenbach, *Phys. Lett.* **118B**, 162 (1982).
11. K. Schreckenbach, G. Colvin, W. Gelletly, and F. von Feilitzsch, *Phys. Lett.* **160B** 325

(1985); A. A. Hahn, K. Schreckenbach, W. Gelletly, F. von Feilitzsch, G. Colvin, and B. Krusche, *Phys. Lett.* **B218**, 365 (1989).
12. H. F. Schopper, *Weak Interactions and Nuclear Beta Decay*, North-Holland, Amsterdam, 1966.
13. A. Sirlin, *Phys. Rev.* **164**, 1767 (1967); A. Sirlin, *Phys. Rev. D* **84**, 014021 (2011).
14. M. Fallot, S. Cormon, M. Estienne, A. Algora, V. M. Bui, *et al.*, *Phys. Rev. Lett.* **109**, 202504 (2012).
15. P. Vogel, *Phys. Rev. D* **29**, 1918 (1984) and private communication.
16. A. C. Hayes, J. L. Friar, G. T. Garvey, Gerard Jungman, G. Jonkmans, *Phys. Rev. Lett.* **112**, 202501 (2014).
17. C. Zemach, *Phys. Rev.* **104**, 1771 (1956).
18. J. L. Friar, *Ann. Phys. (N.Y.)* **122**, 151 (1979).
19. B. R. Holstein, *Phys. Rev. C* **9**, 1742 (1974); J. L. Friar and I. Sick, *Phys. Lett.* **B579**, 285 (2004). Equation (2) of the latter allows conversion between the two results.
20. D. J. Millener, D. E. Alburger, E. K. Warburton, and D. H. Wilkinson, *Phys. Rev C* **26**, 1167 (1982).
21. M. B. Chadwick, *Nucl. Data Sheets* **112**, 2887 (2011).
22. M. A. Kellett , O. Bersillon, R. W. Mills, "The JEFF-3.1/-3.1.1 Radioactive Decay Data and Fission Yields Sub-Libraries," JEFF Report 20, NEA Report No. 6287 (2009).
23. A. A. Sonzogni, T. D. Johnson, and E. A. McCutchan, *Phys. Rev. C* **91**, 011301(R) (2015).
24. The beta-decay database used here was kindly provided to us by the Brookhaven Nuclear Data Group, prior to formal release. The updated nuclei relative to ENDF/B-VII-1.1 are ^{82,82}Ge, ^{82}As, $^{88-91}$Br, ^{90}Kr, $^{91-94,96}$Rb, $^{95,97-99}$Y,^{105}Mo, $^{104-106}$Tc, ^{134,137}Sb, ^{137,138}I, $^{140-142}$Cs, ^{143}Bs, $^{143-145}$La.
25. S. T. Holloway, Toshihiko Kawano, and Peter Möller, *J. Korean Phys. Soc.* **59**, 875 (2011).
26. T. Kawano, P. Moller, and W.B. Wilson, Phys. Rev. C 78, 054601 (2008), and T. Kawano and S. T. Holloway, "CGM: Cascading Gamma-ray and Multiplicity Code Ver. 3," (2010) [unpublished].
27. Weili Zhong (for the Daya Bay collaboration), "Measurement of the Reactor Antineutrino Flux and Spectrum at Daya Bay", Invited talk presented at *ICHEP'14*.
28. Soo-Bong Kim (for the RENO collaboration), "Recent Results from RENO & Future Plan", Talk presented at Fermilab, July 25, 2014, and "Precise Measurement of Reactor Neutrino Spectrum at RENO & Mass Hierarchy at RENO-50", Invited talk presented at workshop *Neutrinos : Recent Developments and Future Challenges*, KIPT, Santa Barbara, November 4, 2014.
29. D. A. Dwyer and T. J. Langford, Phys. Rev. Lett. **114** 012502 (2015).
30. G. A. Cowan, A. Turkevich, C. I. Browne, *Phys. Rev.* **122**, 1286 (1961); G. A. Cowan, B. P. Bayhurst, R. J. Prestwood, *Phys. Rev.* **130**, 2380 (1963); G. A. Cowan, B. P. Bayhurst, R. J. Prestwood, J. S. Gilmore, and G. W. Knobeloch, *Phys. Rev.* **144**, 979 (1966); G. A. Cowan, B. P. Bayhurst, R. J. Prestwood, J. S. Gilmore, and G. W. Knobeloch, *Phys. Rev.* **C2**, 615 (1970).
31. J. A. Wheeler, *Physica* **22**, 1103 (1956).